OSCILLATORY AND STATIONARY FLOW INTO TWO- AND THREE-LAYERED ROTATING SEMI-INFINITE CHANNELS

by

Sverre Holte

ABSTRACT

Linear inviscid theory is utilized to investigate stationary and oscillating flow into a rotating two- and three-layered semi-infinite channel. In the stationary case the solution consists of geostrophic flow plus a geostrophic adjustment region near the inlet with length-scale of the order B/π where B is the width of the channel. In this case an explicit solution is obtained. In the oscillating case the solution consists of the adjustment region plus a train of Kelvin-waves travelling down the channel. Possible applications are river flow into a lake, flow through straits and internal tidal waves.

1. INTRODUCTION

The effect of the earth's rotation on river flow through a lake has been observed both in Norwegian lakes, Stigebrandt (1978), and in North American lakes, Hamblin and Carmack (1978). Laboratory experiments, McClimans (1980) and Nof (1978), have verified the importance of the Coriolis force on the flow into a wide basin. Nof (1978) and Hamblin and Carmack (1978) also have presented mathematical models to describe the geostrophic adjustment of flow into a wide basin. The first is nonlinear and inviscid, and the second is a stream-tube model which includes entrainment.

Our study presents an explicit formula for the geostrophic adjustment of a river flowing into a wide basin when nonlinear and viscous effects can be neglected. A discussion of these assumptions is given in Holte (1984). The solution method applied in our study is similar to Taylor (1922) and allows that the input oscillates. In this case a set of linear equations gives the solution to the problem.

2. BASIC EQUATIONS

We shall consider a three layered fluid with a surface layer with density ρ_1, an intermediate layer with density ρ_2 and a bottom layer with density ρ_3. The mean depth of the layers are H_1, H_2 and H_3 respectively. In the undisturbed state the surface and the interfaces between the layers are horizontal. We choose a Cartesian coordinate system (x,y,z) with the z-axis in the vertical direction and the x- and y-axis along the undisturbed surface.

The displacements of the surface and the upper and lower interfaces between the layers are denoted by ζ_1, ζ_2 and ζ_3 respectively. We shall apply the usual inviscid shallow water approxima-

tion and assume hydrostatic pressure. Hence the linearized equation of motion in the three layers can be written

$$\frac{\partial u_1}{\partial t} - fv_1 = -g \frac{\partial \zeta_1}{\partial x} \tag{2-1a}$$

$$\frac{\partial v_1}{\partial t} + fu_1 = -g \frac{\partial \zeta_1}{\partial y} \tag{2-1b}$$

$$\frac{\partial u_2}{\partial t} - fv_2 = -g \frac{\partial}{\partial x}(\zeta_1+\varepsilon\zeta_2) \tag{2-2a}$$

$$\frac{\partial v_2}{\partial t} + fu_2 = -g \frac{\partial}{\partial y}(\zeta_1+\varepsilon\zeta_2) \tag{2-2b}$$

$$\frac{\partial u_3}{\partial t} - fv_3 = -g \frac{\partial}{\partial x}(\zeta_1+\varepsilon\zeta_2+\varepsilon\zeta_3) \tag{2-3a}$$

$$\frac{\partial v_3}{\partial t} + fu_3 = -g \frac{\partial}{\partial y}(\zeta_1+\varepsilon\zeta_2+\varepsilon\zeta_3) \tag{2-3b}$$

where u_i, v_i $i = 1,2,3$ denote the horizontal velocity components in the three layers respectively, f is the Coriolis parameter, g the acceleration due to gravity and ε the relative density difference. Since the relative density differences between the layers are assumed to be small we have set $(\rho_2-\rho_1)/\rho_2 \simeq (\rho_3-\rho_2)/\rho_3 = \varepsilon$, $\rho_1/\rho_2 \simeq 1$ and $\rho_1/\rho_3 \simeq 1$. By assuming no mixing across the layers the continuity equation for the three layers can be written

$$\frac{\partial \zeta_1}{\partial t} - \frac{\partial \zeta_2}{\partial t} = -\frac{\partial}{\partial x}(u_1 H_1) - \frac{\partial}{\partial y}(v_1 H_1) \tag{2-4}$$

$$\frac{\partial \zeta_2}{\partial t} - \frac{\partial \zeta_3}{\partial t} = -\frac{\partial}{\partial x}(u_2 H_2) - \frac{\partial}{\partial y}(v_2 H_2) \tag{2-5}$$

$$\frac{\partial \zeta_3}{\partial t} = -\frac{\partial}{\partial x}(u_3 H_3) - \frac{\partial}{\partial y}(v_3 H_3) \tag{2-6}$$

For the internal or baroclinic motion the surface displacement is small and we neglect $\frac{\partial \zeta_1}{\partial t}$ compared to $\frac{\partial \zeta_2}{\partial t}$ in equation (2-4). Hence eq. (2-4) reads

$$\frac{\partial \zeta_2}{\partial t} = \frac{\partial}{\partial x}(u_1 H_1) + \frac{\partial}{\partial y}(v_1 H_1) \tag{2-7}$$

and similarly we have

$$\frac{\partial}{\partial x}(u_1 H_1 + u_2 H_2 + u_3 H_3) + \frac{\partial}{\partial y}(v_1 H_1 + v_2 H_2 + v_3 H_3) = 0 \qquad (2\text{-}8)$$

By differentiating with respect to t we may eliminate either u_1 or v_1 from (2-1a) and (2-1b) and we obtain

$$\begin{aligned} Du_1 &= -gD_1\zeta_1 \\ Dv_1 &= -gD_2\zeta_1 \end{aligned} \qquad (2\text{-}9)$$

and from (2-2, a,b) and (2-3, a,b)

$$\begin{aligned} Du_2 &= -gD_1(\zeta_1 + \varepsilon\zeta_2) \\ Dv_2 &= -gD_2(\zeta_1 + \varepsilon\zeta_2) \end{aligned} \qquad (2\text{-}10)$$

and

$$\begin{aligned} Du_3 &= -gD_1(\zeta_1 + \varepsilon\zeta_2 + \varepsilon\zeta_3) \\ Dv_3 &= -gD_2(\zeta_1 + \varepsilon\zeta_2 + \varepsilon\zeta_3 \end{aligned} \qquad (2\text{-}11)$$

where the operators $D \equiv \frac{\partial^2}{\partial t^2} + f^2$, $D_1 = \frac{\partial^2}{\partial x \partial t} + f\frac{\partial}{\partial y}$ and $D_2 = \frac{\partial}{\partial y \partial t} - f\frac{\partial}{\partial x}$. By multiplying (2-9)-(2-11) with H_1, H_2 and H_3 respectively and differentiating with respect to x and y the velocity components can be eliminated by using eqs (2-6)-(2-8) and we finally obtain

$$g(H_1+H_2+H_3)\nabla^2\zeta_1 + \varepsilon g(H_2+H_3)\nabla^2\zeta_2 + \varepsilon g H_3 \nabla^2\zeta_3 = 0 \qquad (2\text{-}12)$$

$$D\zeta_2 + gH_1\nabla^2\zeta_1 = 0 \qquad (2\text{-}13)$$

$$D\zeta_3 - gH_3\nabla^2(\zeta_1 + \varepsilon\zeta_2 + \varepsilon\zeta_3) = 0 \qquad (2\text{-}14)$$

From (2-12)-(2-14) we find

$$\zeta_1 = -\frac{\varepsilon[(H_2+H_3)\zeta_2 + H_3\zeta_3]}{H_1+H_2+H_3}$$

$$D\zeta_2 - \frac{\varepsilon g H_1 \nabla^2[(H_2+H_3)\zeta_2 + H_3\zeta_3]}{H_1+H_2+H_3} = 0$$

$$D\zeta_3 - \frac{\varepsilon g H_3 \nabla^2[(H_1\zeta_2 + (H_1+H_2)\zeta_3]}{H_1+H_2+H_3} = 0$$

If we assume that the bottom layer is very deep compared to the other layers, i.e. $H_3 >> H_1$, H_2, these equations simplify further

$$\zeta_1 = -\varepsilon(\zeta_2+\zeta_3)$$
$$D\zeta_2 - \varepsilon g H_1 \nabla^2(\zeta_2+\zeta_3) = 0$$
$$D\zeta_3 - \varepsilon g \nabla^2[H_1\zeta_2+(H_1+H_2)\zeta_3] = 0$$

The latter two equations possess solutions of the form $\zeta_2 = q\zeta_3$ where q is a constant and both ζ_2 and ζ_3 are determined by the equation

$$(D-c^2\nabla^2)(\zeta_2,\zeta_3) = 0 \qquad (2\text{-}15)$$

where $c^2 = \varepsilon g H_1(1 + \frac{1}{q})$. The constant q has two different values

$$q_{1,2} = -\frac{1}{2}\frac{H_2}{H_1} \pm \sqrt{1 + \frac{1}{4}(\frac{H_2}{H_1})^2} \qquad (2\text{-}16)$$

The positive value, q_1, corresponds to vertical deflection of the middle layer while the negative value, q_2, corresponds to stretching and thickening of the middle layer. Table 1 shows values of q_1 and q_2 together with the corresponding values of the velocities $c_i = [\varepsilon g H_1(1 + \frac{1}{q_i})]^{\frac{1}{2}}$, $i = 1,2$.

Table 1

$\frac{H_2}{H_1}$	q_1	q_2	$\frac{c_1}{\sqrt{\varepsilon g H_1}}$	$\frac{c_2}{\sqrt{\varepsilon g H_1}}$
0	1	-1	1.41	0
0.1	0.95	-1.05	1.43	0.22
0.5	0.78	-1.28	1.51	0.47
1.0	0.62	-1.62	1.62	0.62
2.0	0.41	-2.41	1.85	0.76
3.0	0.30	-3.30	2.08	0.83
10.0	0.10	-10.1	3.31	0.95

In cases with a deep bottom layer where eq. (2-15) applies it is possible to show that both the velocity components in the intermediate layer u_2 and v_2 satisfy a corresponding equation. We have $\zeta_1 + \varepsilon\zeta_2 = -\varepsilon\zeta_3$ and by differentiating (2-10) and invoking (2-15) we find

$$(D-c^2\nabla^2)(u_2,v_2) = 0 \qquad (2\text{-}17)$$

Similar equations for a two layer model are obtained by taking the limit $H_2 \to 0$ which leads to $q_{1,2} = \pm 1$. In this case only the positive value has a physical meaning and we set $\zeta_2=\zeta_3=\zeta$. Hence

$$(D-c^2\nabla^2)\zeta = 0 \qquad (2\text{-}18)$$

where $c^2 = 2\varepsilon g H_1$. We also have

$$\zeta_1 = -2\varepsilon\zeta_2 \qquad (2\text{-}19)$$

The factor 2ε occurs since we by taking the limit $H_2 \to 0$ obtain a two-layered model with relative density difference 2ε. In a similar way as described above it can be shown that the velocity components u_1 and v_1 in the surface layer satisfy the equation

$$(D-c^2\nabla^2)(u_1,v_1) = 0 \qquad (2\text{-}20)$$

3. FLOW INTO A LONG RECTANGULAR TWO-LAYERED BASIN

In this work we shall consider situations where the inflow is at one end of the basin. The x-axis is oriented along the longitudinal axis with the origo at the inlet and the lateral side-walls have coordinates $y = \pm b/2$ where b is the width of the basin. We shall first examine the case where the flow enters the surface layer of a two-layered basin with a deep bottom layer. In this case eqs (2-18) and (2-20) apply and we introduce dimensionless coordinates

$$\eta = 2x/b, \quad \xi = 2y/b,$$

Hence eq. (2-20) can be rewritten

$$\left(\left(\frac{b}{2c}\right)^2 \frac{\partial^2}{\partial t^2} + \alpha^2 - \frac{\partial^2}{\partial \eta^2} - \frac{\partial^2}{\partial \xi^2}\right)(u_1, v_1) = 0 \tag{3-1}$$

where the parameter $\alpha = fb/2c$ and $c = \sqrt{2\varepsilon g H_1}$. The boundary conditions at the side walls $\xi = \pm 1$ are

$$v_1 = 0 \tag{3-2}$$

Although stationary inflow will be most relevant for the application we shall allow for the possibility that the inflow may vary in time. Hence the inflow is specified as a periodic function

$$u_1 = \hat{u}_0(\xi) e^{i\omega t} \tag{3-3}$$

at the end of the basin i.e. for $\eta = 0$. ω is the angular velocity and steady state solutions are obtained by taking the limit $\omega \to 0$.

Eq. (3-1) has solutions of the form

$$u_1 = \hat{u}_1(\eta, \xi) e^{i\omega t}$$

$$v_1 = \hat{v}_1(\eta, \xi) e^{i\omega t}$$

where

$$\hat{u}_1 = -A_0 e^{-\alpha\xi} e^{-ip\eta} - \sum_{n=1}^{\infty} A_n [\lambda_n \beta_n C_n(\xi) + i\alpha p S_n(\xi)] e^{-\beta_n \eta} \tag{3-4}$$

$$\hat{v}_1 = \sum_{n=1}^{\infty} A_n (\lambda_n^2 + \alpha^2) S_n(\xi) e^{-\beta_n \eta} \tag{3-5}$$

Here $p = \omega b/2c$.

The corresponding displacement of the interface between the surface and the bottom layer is

$$\zeta_2/H_1 = \frac{A_0}{c} e^{-\alpha\xi} e^{-ip\eta} + \sum_{n=1}^{\infty} \frac{A_n}{c} [ip\lambda_n C_n(\xi) + \alpha\beta_n S_n(\xi)] e^{-\beta_n \eta} \tag{3-6}$$

$A_0, A_1, \ldots, A_n$ are integration constants and the functions $C_n(\xi)$ and $S_n(\xi)$ are defined by

$$C_n(\xi) = \cos \lambda_n(1-\xi)$$
$$S_n(\xi) = \sin \lambda_n(1-\xi)$$

The boundary conditions at the side walls are satisfied with $\lambda_n = n\pi/2$. The parameter β_n is given by

$$\beta_n^2 = \lambda_n^2 + \alpha^2 - p^2$$

We are mainly interested in long periodic variation of the inflow when β_n can be assumed real. Our solution method then has a cut-off frequency

$$\omega_0 = (f^2 + \frac{\pi^2 c^2}{B^2})^{\frac{1}{2}}.$$

The cut-off frequency ω_0 is of the same order of magnitude as the Coriolis parameter f in most geophysical applications. The integration constants are determined by the inflow condition (3-3) which requires

$$A_0 e^{-\alpha\xi} + \sum_{n=1}^{\infty} A_n[\lambda_n\beta_n C_n(\xi)+i\alpha p S_n(\xi)] = - \hat{u}_0(\xi) \qquad (3\text{-}7)$$

The constants $A_0, A_1, \ldots, A_n$ can be found from eq. (3-7) by replacing $e^{-\alpha\xi}$, $S_n(\xi)$ and $\hat{u}_0(\xi)$ with their Fourier-series in $C_n(\xi)$, Taylor (1921). Alternatively eq. (3-7) can be multiplied by $C_n(\xi)$ $n = 0,1,2,\ldots$ and integrated from $\xi = -1$ to $\xi = 1$. The methods are identical and lead to a set of linear equations for the unknown quantities.

In general A_n $n = 0,1,\ldots$ are complex which reflects a phase-shift between the inflow and the flow in the basin. We put

$$A_n = a_n + i\, b_n \qquad n = 0,1,\ldots \qquad (3\text{-}9)$$

We can define the phase-shift as $\delta = -\text{arc tan}\,(b_0/a_0)$. The resulting equations for a_n and b_n can then be written

$$- \frac{\sinh \alpha}{\alpha} a_0 + \sum_{k \text{ odd}} \alpha p b_k \frac{2}{k\pi} = \gamma_0 \qquad (3\text{-}10)$$

k odd (k even)

$$-\frac{4\alpha}{\pi^2}\chi_k a_0 - \lambda_k\beta_k a_k + \alpha p \sum_{\substack{l \text{ even} \\ (l \text{ odd})}} \frac{4l}{\pi} t_{lk} b_l = \gamma_k \qquad (3\text{-}11)$$

$$-\frac{\sinh\alpha}{\alpha} b_0 - \sum_{k \text{ odd}} \alpha p \frac{2}{k\pi} a_k = 0 \qquad (3\text{-}12)$$

k odd (k even)

$$-\frac{4\alpha}{\pi^2}\chi_k b_0 - \lambda_k\beta_k b_k + \alpha p \sum_{\substack{l \text{ even} \\ (l \text{ odd})}} \frac{4l}{\pi} t_{lk} a_l = 0 \qquad (3\text{-}13)$$

In these equations we have introduced the quantities

$$\chi_n = \frac{(-1)^n e^{\alpha} - e^{-\alpha}}{(4\alpha^2/\pi^2)+n^2}$$

$$t_{nm} = (n^2-m^2)^{-1}$$

γ_n - coefficients in the series for $\hat{u}_0(\xi)$

We note that when the inflow is stationary, i.e. $p = 0$, eqs (3-10)-(3-13) give explicit expressions for the unknown a_n whereas $b_n \equiv 0$. In this case

$$a_0 = -\frac{\gamma_0\alpha}{\sinh\alpha}$$
$$a_n = \frac{-\gamma_n - (4\alpha/\pi^2)\chi_n a_0}{\lambda_n\beta_n} \qquad (3\text{-}14)$$

The flow in the basin is now described by

$$\hat{u}_1 = -a_0 e^{-\alpha\xi} - \sum_{n=1}^{\infty} a_n\lambda_n\beta_n C_n(\xi) e^{-\beta_n\eta} \qquad (3\text{-}15)$$

$$\hat{v}_1 = \sum_{n=1}^{\infty} a_n(\lambda_n^2+\alpha^2) S_n(\xi) e^{-\beta_n\eta} \qquad (3\text{-}16)$$

The first term in $\hat{u}_1$, namely $-a_0 e^{-\alpha\xi}$, describes geostrophic motion which is present for all positive values of x.

The contribution from the series in eqs (3-15) and (3-16) diminishes rapidly away from the inlet and the e-folding distance for the dominant term is $\eta = 2/\pi$. This shows that the geostrophic

adjustment takes place over a remarkably short length scale of order b/π, see fig. 4.

The general solution of eqs (3-10)-(3-13) describes Kelvin-waves with frequency ω that travel along the right-hand side of the channel. In a region near the inlet with length of the order b/π the flow adjusts from the prescribed inflow to this train of Kelvin-waves, see fig. 5.

We can now find the flow for various input conditions simply by replacing γ_k with the appropriate series in eqs (3-10)-(3-13) in the oscillatory case or in eq. (3-14) in the stationary case respectively.

A first approximation to river flow into a lake or flow through straits is to prescribe $\hat{u}_0(\xi)$ as a box-profile:

$$\hat{u}_0(\xi) = u_0 \quad |\xi| < 1$$
$$\hat{u}_0(\xi) = 0 \quad 1 < |\xi| < 1$$

The coefficients γ_k then become

$$\gamma_0 = u_0 l$$
$$\gamma_n = -\frac{2u_0}{\lambda_n} \cos \lambda_n \sin l\lambda_n \qquad (3\text{-}17)$$

The solutions are linear in u_0 and in the computations we have put $u_0=1$. This corresponds to a scaling of the results with u_0/c.

In figs 1, 2 and 3 we have displayed the dependence of the motion far downstream, given by a_0 and b_0, on α, l and ω. The solution for stationary flow is given by eq. (3-14), and in this case a_0 is a linear function of l, see fig. 2. a_0 decreases with increasing α, see fig. 1. The amplitude of the thermocline displacement ζ_2 is $a_0 e^{\alpha}$, however, and an increase in α must be compensated by a decrease in a_0. The thermocline displacement ζ_2 is shown in fig. 4 for $\alpha = 2$ and $l = 0.2$. The rapid geostrophic

adjustment is clearly revealed. The resemblance with fig. 10.7c in Gill (1982) should be noted.

When the input oscillates, the motion in the channel is out of phase with the input. The phase-angle δ increases with increasing α and ω. In the case depicted in fig. 1, the phase-angle δ is small for $\alpha \leq 1$ and it inceases to $\delta \simeq \pi$ for $\alpha = 4$. The motion grows fast out of phase when ω increases. The phase-angle δ increases almost linearly with ω and $\delta \simeq \pi/2$ for $\omega = f$ when $\alpha = 2$ and $l = 0.2$, see fig. 3.

Fig. 3 shows a feature in the oscillating case which is not present in the stationary case. The increase of a_0 and b_0 with l is slower than linear when $\omega \neq 0$. This reflects that even though more water oscillates back and forth near the inlet when l increases, this does not lead to a proportional increase in the amplitude in the Kelvin-waves far down-stream. a_0 is a linear function of l when $\omega = 0$ as has been pointed out.

The solution converges fast both in the stationary case and in the oscillating case, see table 2. The convergence in the stationary case is given explicitly in eqs (3-14)-(3-16). The convergence in the oscillating case closely follows the stationary case. In our computations we have used $N = 10$ terms in the series for u and v. A change in N yields no change in the leading terms.

4. FLOW INTO A THEREE-LAYERED BASIN

We now consider flow into a three-layered basin. We utilize the analysis from the two-layer case since the governing equations in the two cases are similar. There is one typical wave-velocity, $c = (2\varepsilon gH)^{\frac{1}{2}}$, present in the two-layer case. In the three-layer case, however, two velocities are present

$$c_{1,2} = [\varepsilon g H_1 (1 + \frac{1}{q_{1,2}})]^{\frac{1}{2}} \qquad (4\text{-}1)$$

where $q_{1,2}$ is given by eq. (2-16).

The inflow must be specified for both the middle and upper layers,

$$\begin{aligned} u_1 &= \bar{u}_0(\xi)e^{i\omega t} \\ & \qquad \eta = 0 \\ u_2 &= \hat{u}_0(\xi)e^{i\omega t} \end{aligned} \qquad (4\text{-}2)$$

We shall assume submerged inflow, i.e. $\bar{u}_0 = 0$ and

$$\begin{aligned} \hat{u}_0(\xi) &= u_0 \quad |\xi| < 1 \\ \hat{u}_0(\xi) &= 0 \quad 1<|\xi|<1 \end{aligned}$$

The motion has two modes connected to q_1 and q_2 respectively,

$$\begin{aligned} \zeta_2^{(1)} &= q_1 \zeta_3^{(1)} \\ \zeta_2^{(2)} &= q_2 \zeta_3^{(2)} \end{aligned} \qquad (4.3)$$

The velocities in the upper and the middle layers are for each mode related through eq. (4-3) and the equation of continuity:

$$\frac{\partial \zeta_2}{\partial t} = H_1 (\frac{\partial u_1}{\partial x} + \frac{\partial v_1}{\partial y}) \qquad (4\text{-}4)$$

$$\frac{\partial \zeta_3}{\partial t} = H_1 (\frac{\partial u_1}{\partial x} + \frac{\partial v_1}{\partial y}) + H_2 (\frac{\partial u_2}{\partial x} + \frac{\partial v_2}{\partial y}) \qquad (4\text{-}5)$$

For each mode in each layer the expressions (3-4) and (3-5) can be used for the velocities. The complex numbers $A_0, A_1, \ldots$ are replaced as follows:

$a_j + i\, b_j$	for	q_1	mode	middle layer
$d_j + i\, e_j$	"	q_2	"	"
$A_j + i\, B_j$	"	q_1	"	upper "
$D_j + i\, E_j$	"	q_2	"	"

Invoking eqs (4-3)-(4-5) gives

$$(A_j,B_j) = r_1(a_j,b_j) \tag{4-6}$$

$$(D_j,E_j) = r_2(d_j,e_j) \tag{4-7}$$

where

$$r_i = \frac{q_i H_2}{(1-q_i)H_1} \qquad i = 1,2$$

The velocities at $\eta = 0$ can then be written

middle layer

$$\begin{aligned}\hat{u}_2 = &-a_0 e^{-\alpha_1 \xi} - \sum_{n=1}^{\infty} (a_n \lambda_n \beta_{1n} C_n - \alpha_1 p_1 b_n S_n) \\ &-ib_0 e^{-\alpha_1 \xi} - i\sum_{n=1}^{\infty} (b_n \lambda_n \beta_{1n} C_n + \alpha_1 p_1 a_n S_n) \\ &-d_0 e^{-\alpha_2 \xi} - \sum_{n=1}^{\infty} (d_n \lambda_n \beta_{2n} C_n - \alpha_2 p_2 e_n S_n) \\ &-ie_0 e^{-\alpha_2 \xi} - i\sum_{n=1}^{\infty} (e_n \lambda_n \beta_{2n} C_n + \alpha_2 p_2 d_n S_n)\end{aligned} \tag{4-8}$$

$\hat{v}_2$ - correspondingly

upper layer

same as middle layer, only a_n, b_n, d_n and e_n are replaced by $r_1 a_n$, $r_1 b_n$, $r_2 d_n$ and $r_2 e_n$.

The subscripts 1 and 2 in α_1, α_2 p_1, p_2, β_{1n} and β_{2n} relate these quantities to the q_1- and q_2-mode respectively.

By the same procedure as in the two-layer case we get the following set of equations for a_n, b_n, d_n and e_n:

middle layer

$$\begin{aligned}&-\frac{\sinh \alpha_1}{\alpha_1} a_0 - \frac{\sinh \alpha_2}{\alpha_2} d_0 \\ &+ \sum_{k\ \mathrm{odd}} \alpha_1 p_1 b_k \frac{2}{k\pi} + \sum_{k\ \mathrm{odd}} \alpha_2 p_2 e_k \frac{2}{k\pi} = \gamma_0\end{aligned} \tag{4-9}$$

k odd (k even)

$$-\frac{4\alpha_1}{\pi^2}\chi_{1k}a_0 - \frac{4\alpha_2}{\pi^2}\chi_{2k}d_0 - \lambda_k\beta_{1k}a_k - \lambda_k\beta_{2k}d_k$$
$$+\sum_{\substack{l \text{ even}\\(l \text{ odd})}}\frac{4l}{\pi}t_{lk}(\alpha_1 p_1 b_l + \alpha_2 p_2 e_l) = \gamma_k \qquad (4\text{-}10)$$

$$-\frac{\sinh\alpha_1}{\alpha_1}b_0 - \frac{\sinh\alpha_2}{\alpha_2}e_0$$
$$-\sum_{k \text{ odd}}\alpha_1 p_1 \frac{2}{k\pi}a_k - \sum_{k \text{ odd}}\alpha_2 p_2 \frac{2}{k\pi}d_k = 0 \qquad (4\text{-}11)$$

k odd (k even)

$$-\frac{4\alpha_1}{\pi^2}\chi_{1k}b_0 - \frac{4\alpha_2}{\pi^2}\chi_{2k}e_0 - \lambda_k\beta_{1k}b_k - \lambda_k\beta_{2k}e_k$$
$$-\sum_{\substack{l \text{ even}\\(l \text{ odd})}}\frac{4l}{\pi}t_{lk}(\alpha_1 p_1 a_l + \alpha_2 p_2 d_l) = 0 \qquad (4\text{-}12)$$

upper layer

same as middle layer, only a_n, b_n, d_n and e_n are replaced by $r_1 a_n$, $r_1 b_n$, $r_2 d_n$, $r_2 e_n$ respectively. The right-hand side equals zero in all equations.

In the calculations we have put $u_0 = 1$ which corresponds to a scaling of the results with u_0/c_0 where $c_0 = (\varepsilon g H_1)^{\frac{1}{2}}$. It should be noted that $c_2 < c_0$ and $c_1 > c_0$ always. A criterion for the linearization of the basic equations is $u_0/c_2 \ll 1$ which may be much stronger than $u_0/c_0 \ll 1$ when $H_2/H_1 \ll 1$, see table 1.

When $\omega \neq 0$ the motion far down-stream consists of two Kelvin wave-trains moving with velocity c_1 and c_2 respectively. The Kelvin waves cause vertical deflection (q_1-mode) and stretching and thickening (q_2-mode) of the intermediate layer.

In fig. 6 we have shown how the amplitude of the two wave-trains vary when the effect of the earth's rotation increases. This effect is measured by the parameter $\alpha_0 = \frac{fb}{2c_0}$. Since $c_1 > c_0$ and

$c_2 < c_0$ we have $\alpha_1 < \alpha_0$ and $\alpha_2 > \alpha_0$. The rotation of the earth is therefore more strongly felt by the q_2-mode than by the q_1-mode. One notes the similarity between the curves for the q_2-mode (d_0, e_0) in fig. 6 and the corresponding curves in the two-layer case, see fig. 1. The q_1-mode (a_0, b_0) has a much weaker dependence on α_0 - reflecting that the Coriolis force has not come fully into play for this mode. The curves for a_0 and b_0 are indeed similar to those for d_0 and e_0 respectively, only the α_0-axis must be stretched. The phase angle for the two modes shows dependence on α_0 similar to the two-layer case after stretching of the α_0-axis for the q_1-mode and narrowing for the q_2-mode.

An increase in the width of the inlet, 21, does not lead to a proportional increase in the amplitude for the two modes. With $\alpha_0 = 2$ (corresponding to $\alpha_1 = 1.24$ and $\alpha_2 = 3.24$) and $\omega = f$, a_0 and b_0 depend almost linearly on l whereas d_0 and e_0 increases for $l < 0.4$ and decreases for $l > 0.4$, see fig. 7. For $l \approx 0.82$ the q_2-mode is not excited at all. In the absence of rotation, i.e. when $f = 0$, the amplitude of the downstream waves will depend linearly on l. The more complicated dependence when $f \neq 0$ is possible since in this case the motion in the channel may be out of phase with the inflow.

The q_1-mode is only slightly out of phase for different choices of ω when $\alpha_0 = 2$ and $l = 0.2$, see fig. 8. The q_2-mode, however, grows fast out of phase when ω increases. Again this can be related to the slower phase-speed for the q_2-mode which implies that the earth's rotation is more stronly felt for this mode.

As can be seen from figs 6-8, the two modes are of the same order of magnitude for most choices of ω, l and α_0. The relative magnitude of the two modes may, however, vary as a function of the ratio H_2/H_1. In fig. 9 we have displayed a_0, d_0 and e_0 as

functions of H_2/H_1 when $\omega = f$ and $\alpha_0 = 0.5$, i.e. the effect of rotation is weak. In this case b_0 is close to zero for all H_2/H_1. The q_2-mode is the greater for $H_2/H_1 < 1$ and the q_1-mode is the greater for $H_2/H_1 >> 1$, i.e. when the upper layer is shallow compared to the intermediate layer. For larger values of α_0, d_0 and e_0 become small. The q_2-mode may still be significant though, since the amplitudes for this mode are $d_0 e^{\alpha_2}$ and $e_0 e^{\alpha_2}$.

The convergence is typically shown in table 2. The convergenc- rate is about the same as in the two-layer case and the leading terms are independent of a variation of the number N of terms in the series. In the computations displayed, we have put $N = 10$.

5 STATIONARY FLOW INTO A THREE-LAYERED BASIN

Solution when the inflow is steady is not obtained by letting $p_1, p_2 \to 0$ in eqs (4-9)-(4-12). In the stationary case there shall be no motion in the upper layer as long as the inflow is in the intermediate layer. In the solutions obtained in sect.4, the velocities in the upper and middle layers are coupled and there will be motion in the upper layer also for $p_1 = p_2 = 0$. Stationary flow in a three-layered channel must therefore be treated specially. In this case $\zeta_1 = 0$ since there is no motion in the upper layer. From $\zeta_1 + \varepsilon\zeta_2 + \varepsilon\zeta_3 = 0$ follows $\zeta_2 = -\zeta_3$. Conservation of potential vorticity yields

$$f + \frac{\partial v_2}{\partial x} - \frac{\partial u_2}{\partial y} = \frac{f}{H_2}(H_2 + \zeta_2 - \zeta_3) \tag{5-1}$$

The equations for the horizontal motion in this case read

$$-fv_2 = -\varepsilon g \frac{\partial \zeta_2}{\partial x} \tag{5-2}$$

$$fu_2 = -\varepsilon g \frac{\partial \zeta_2}{\partial y} \tag{5-3}$$

By combining (5-1)-(5-3) we get

$$f^2\zeta_3 - \frac{1}{2}\varepsilon g H_2 \nabla^2 \zeta_3 = 0 \tag{5-4}$$

Equation (5-4) corresponds to e.g. eq.(2-15) with $\frac{\partial}{\partial t} = 0$ and $c = (\frac{1}{2}\varepsilon g H_2)^{\frac{1}{2}}$. We note that this quantity is independent of H_1 and therefore principally different from the corresponding velocities c_1 and c_2 in the time-dependent case.

The velocities in the intermediate layer can then be written

$$u_2 = -a_0 e^{-\alpha\xi} - \sum_{n=1}^{\infty} a_n \lambda_n \beta_n C_n(\xi) e^{-\beta_n \eta} \tag{5-5}$$

$$v_2 = \sum_{n=1}^{\infty} a_n (\lambda_n^2 + \alpha^2) S_n(\xi) e^{-\beta_n \eta} \tag{5-6}$$

where

$$a_0 = -\frac{\gamma_0 \alpha}{\sinh \alpha}$$
$$a_n = \frac{-\gamma_n - (4\alpha/\pi^2)\chi_n a_0}{\lambda_n \beta_n} \tag{5-7}$$

with the new value for c in the appropriate places. This follows from arguments similar to those given in the stationary two-layer case, see sect. 3. The results obtained in the stationary two-layer case are therefore valid also for stationary flow into a three-layered channel.

CONCLUSION

In absence of rotation the waves in the channel will be in phase with the inflow ($\delta = 0$) and the amplitudes will depend linearly on the inlet width $2l$. The amplitudes will also be independent of the frequency ω of the inflow. This can be seen e.g. by putting $\alpha = 0$ in eqs (3-10)-(3-13). When rotation is

introduced, none of this is true. In a wide rotating channel fluid near the inlet will have a velocity component normal to the channel axis because of the Coriolis force. The motion in the channel may therefore be out of phase with the inflow and the response of the channel to the prescribed inflow then becomes more complex than in the non-rotating case.

The response when the channel rotates has been determined analytically in this work. The analysis is based upon linearization and that viscous effects may be neglected. The solution is therefore not valid close to a river inlet where mixing processes may be strong and the river water forms a well-defined plume. This inlet region must be excluded from the domain, see Holte (1984) for a discussion. The prescribed flow into the channel in this study is the flow-pattern down-stream from the inlet mixing region.

Bottom and interface friction and background turbulence in the channel may also affect the flow even when they are weak, see Holte (1984) in the stationary case and Martinsen and Weber (1981) when the inflow oscillates. From the discussion in the latter study one may question whether the q_2-mode in the three-layer case is generated at all in most circumstances.

The geophysically most interesting part of the paper is the results for stationary flow since it covers a variety of flow phenomena, e.g. river flow into a lake or a fjord, ocean currents through straits or waste-water outlets. The motion when $\omega \neq 0$ may describe internal tidal waves generated e.g. over fjord sills.

ACKNOWLEDGEMET

I am most grateful to Dr. Bjørn Gjevik who posed the problem. The work was supported by the Royal Norwegian Council for Scientific and Industrial Research (NTNF).

REFERENCES

Gill, A.E. 1982. Atmosphere-Ocean Dynamics, Academic Press, New York, 662 pp.

Hamblin, P.F. and Carmack, E.C. 1978. River-induced currents in a fjord lake. J.Geophys.Res. 83, 885-899.

Holte, S 1984. Numerical experiments with a three-dimensional model of an enclosed basin. In publication J.Cont.Shelf Res.

Martinsen, E.A. and Weber, J.E. 1981. Frictional influence on internal Kelvin waves. Tellus, 33, 402-410.

McClimans, T.A. 1980. River plume studies in a rotating basin. Report nr. 2-80043, Norwegian Hydrodynamical Laboratories, Trondheim.

Nof, D. 1978. On geostrophic adjustments in sea straits and wide estuaries: Theory and laboratory experiments. Part II - Two-layer system. J.Phys.Oceanogr. 8, no. 5, 861-872.

Stigebrandt, A. 1978. Dynamics of an ice covered lake. Nordic Hydrology, 9, 219-244.

Taylor, G.I. 1922. Tidal oscillations in gulfs and rectangular basins. Proc.Lond.Math.Soc. 20, 148-181.

n	Stationary	Oscillating	
	a_n	a_n	b_n
0	-0.11	-0.04	0.1
1	-0.06	-0.07	0.05
2	0.04	0.04	-0.02
3	-0.003	10^{-4}	0.007
4	-0.006	-0.008	-0.001
5	10^{-4}	10^{-5}	10^{-4}
6	0.002	0.002	10^{-4}
7	10^{-4}	10^{-5}	10^{-4}
8	10^{-4}	10^{-4}	10^{-5}
9	10^{-5}	10^{-6}	10^{-5}
10	10^{-5}	10^{-6}	10^{-5}

Table 2. Convergence of the solution in the two-layer case. $\alpha = 2$, $l = 0.2$. $\omega = f$ in the oscillating case.

n	q_1-mode		q_2-mode	
	a_n	b_n	d_n	e_n
0	-0.05	10^{-4}	-0.13	0.014
1	-0.006	10^{-4}	-0.04	-0.002
2	0.01	10^{-5}	0.03	-0.001
3	10^{-5}	10^{-5}	10^{-4}	10^{-4}
4	-0.002	10^{-6}	-0.005	10^{-5}
5	10^{-6}	10^{-7}	10^{-5}	10^{-6}
6	10^{-4}	10^{-7}	0.002	10^{-5}
7	10^{-6}	10^{-7}	10^{-5}	10^{-5}
8	10^{-4}	10^{-8}	10^{-4}	10^{-6}
9	10^{-7}	10^{-8}	10^{-6}	10^{-6}
10	10^{-7}	10^{-8}	10^{-6}	10^{-6}

Table 3. Convergence of the solution in the three-layer case. $\alpha_0 = 0.5$, $\omega = f$, $l = 0.2$, $H_2/H_1 = 1$.

FIGURE CAPTIONS

Fig. 1 $-a_0$ (1 - stationary, 2 - oscillating) and b_0 (3) as functions of α in the two-layer case. $l = 0.2$. $\omega = f$ in the oscillating case. The phase angle (4) downstream in the oscillating case.

Fig. 2 $-a_0$ (1 - stationary, 2 - oscillating) and b_0 (3) as functions of l in the two-layer case. $\alpha = 2$. $\omega = f$ in the oscillating case.

Fig. 3 $-a_0$ (1) and b_0 (2) as functions of ω in the two-layer case. $\alpha = 2$ and $l = 0.2$. The curve 3 gives the phase angle downstream. ω_0 is the cut-off frequency.

Fig. 4 Thermocline displacement (ζ_2) for stationary flow into a two-layered channel. $\alpha = 2$. $l = 0.2$. Scaled by H_1.

Fig. 5 Thermocline displacement (ζ_2) for oscillating flow into a two-layered channel. $\omega = f$, $\alpha = 2$. $l = 0.2$. Contour interval: 0.1. Scaled by H_1.

Fig. 6 $-a_0$ (1), b_0 (2), $-d_0$ (3) and e_0 (4) as functions of α_0. $l = 0.2$, $\omega = f$ and $H_2/H_1 = 1$.

Fig. 7 $-a_0$ (1), b_0 (2), d_0 (3) and e_0 (4) as functions of l. $\omega = f$, $\alpha_0 = 2$ and $H_2/H_1 = 1$.

Fig. 8 $-a_0$ (1), b_0 (2), $-d_0$ (3) and e_0 (4) as functions of ω. $l = 0.2$, $\alpha_0 = 2$ and $H_2/H_1 = 1$.

Fig. 9 $-a_0$ (1), $-d_0$ (3) and e_0 (4) as functions of H_2/H_1. $l = 0.2$, $\omega = f$ and $\alpha_0 = 0.5$. $b_0 \sim 10^{-4}$ in this case.

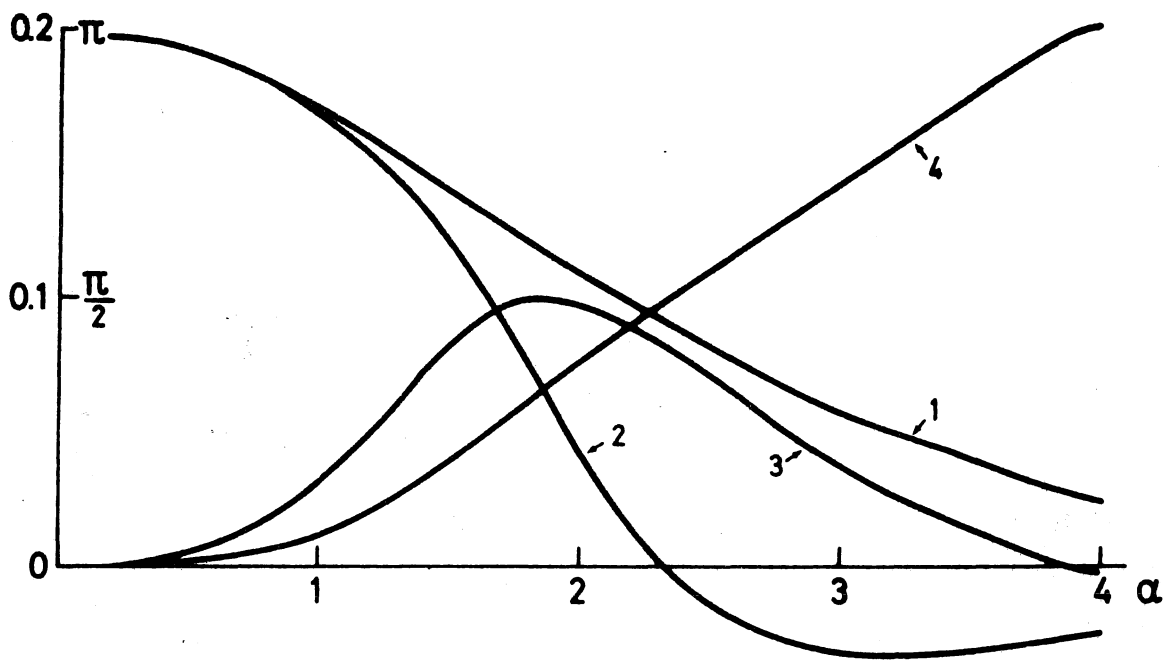

Fig. 1

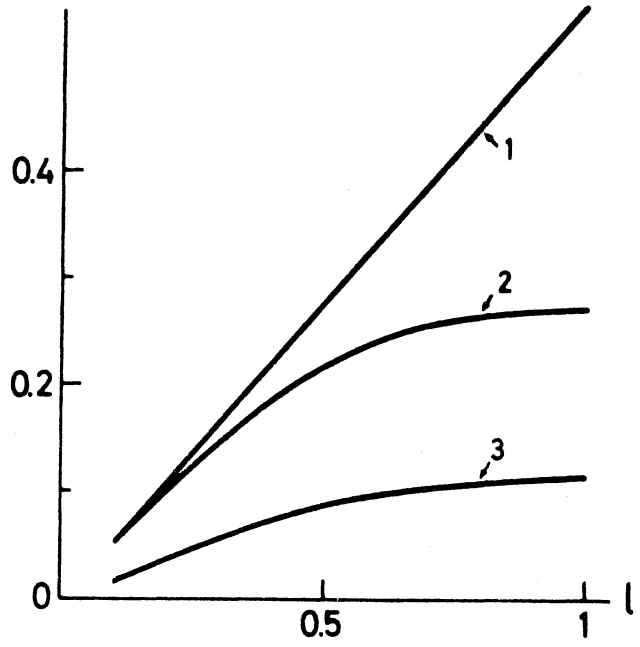

Fig. 2

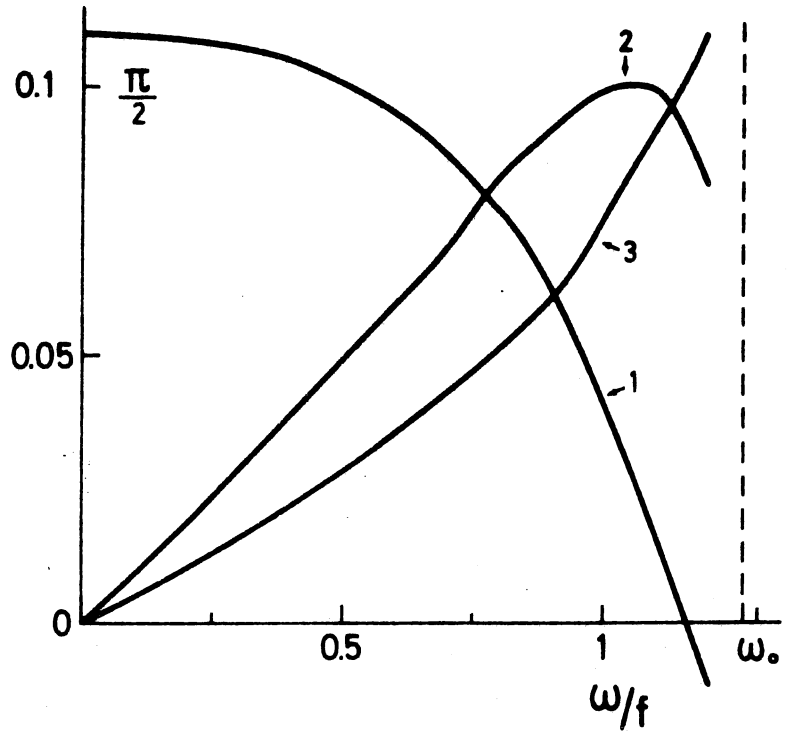

Fig. 3.

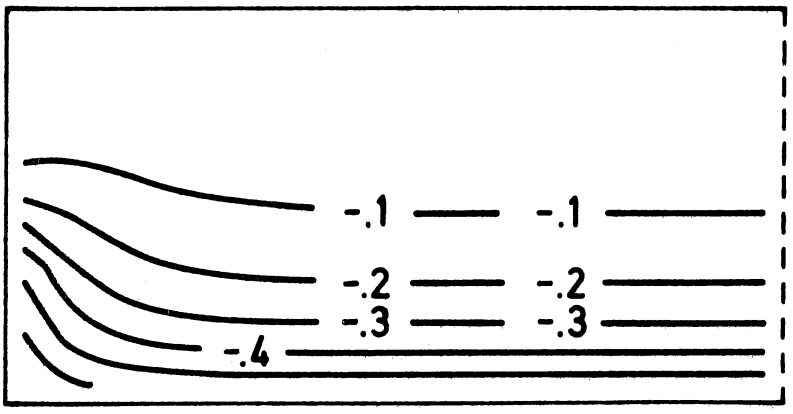

Fig. 4.

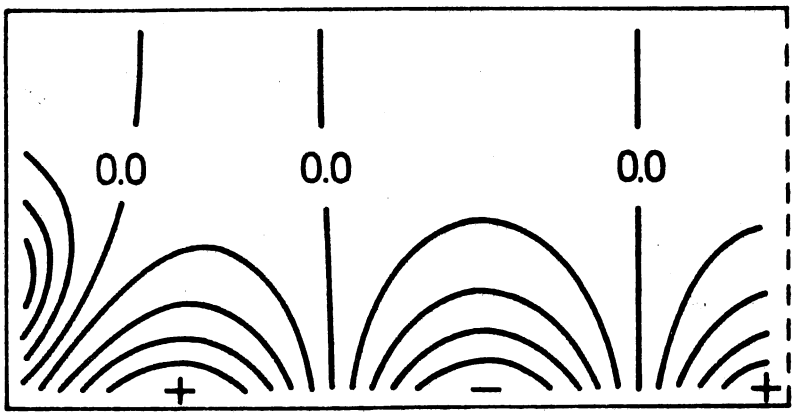

Fig. 5.

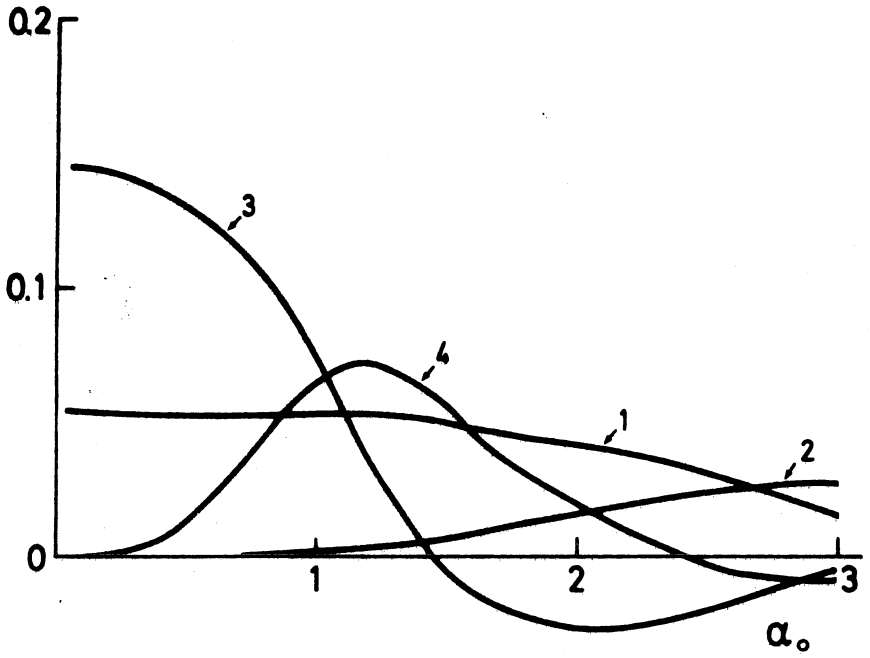

Fig. 6.

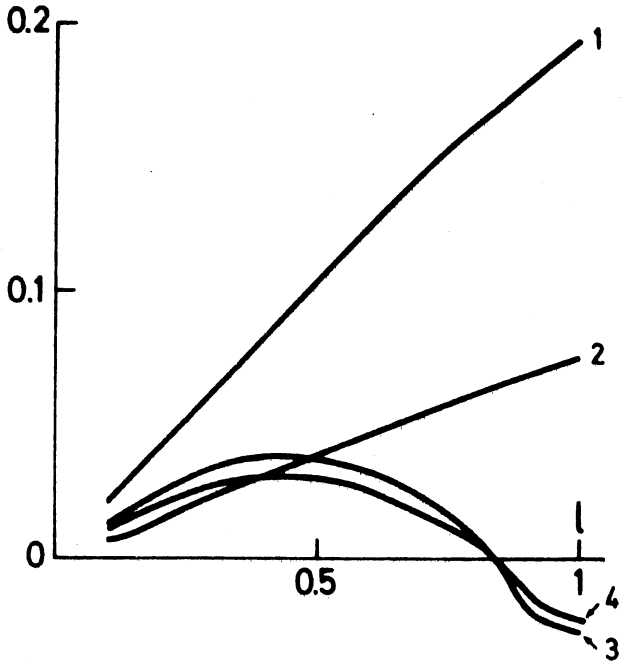

Fig. 7.

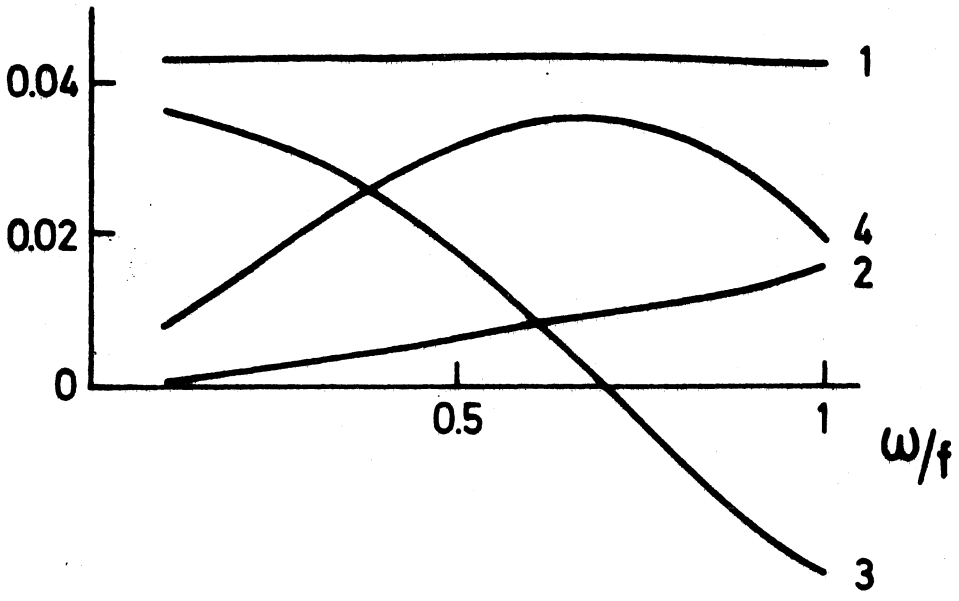

Fig. 8.

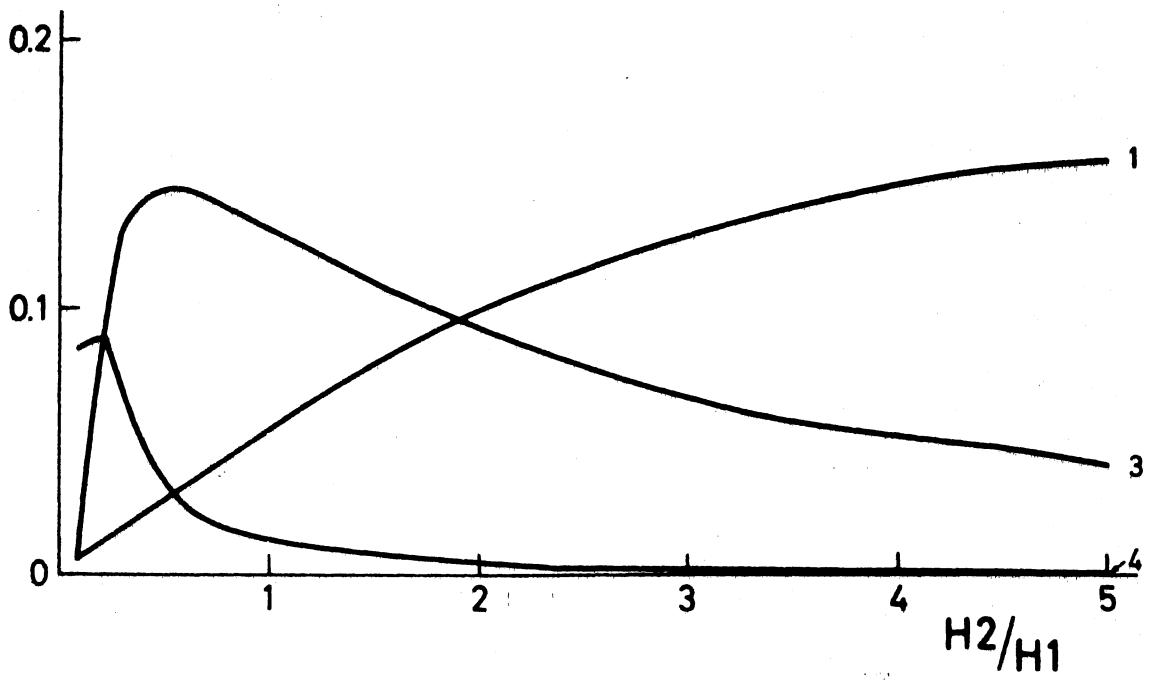

Fig. 9.